10.1109/ULTSYM.2009.0436

Use of quantitative ultrasound to detect temperature variations in biological phantoms due to heating

Goutam Ghoshal and Michael L. Oelze
Bioacoustic Research Laboratory
Department of Electrical and Computer Engineering
University of Illinois at Urbana-Champaign
Urbana, IL 61801
Email: gghoshal@illinois.edu, oelze@uiuc.edu

***Abstract*—High intensity focused ultrasound (HIFU) is a noninvasive technique that has great potential for improving thermal therapies. To target specified regions accurately for treatment, a robust imaging technique is required to monitor HIFU application. Therefore, the development of an ultrasonic imaging technique for monitoring HIFU treatment is highly medically significant. Quantitative ultrasound (QUS) is a novel imaging technique that may improve monitoring of HIFU treatment by quantifying tissue changes. Ultrasonic backscatter experiments were performed on two types of phantoms to understand the variations in QUS parameters with increases in temperature from 36 to $50^{\circ}\mathrm{C}$. The phantoms were biological phantoms made of agar and containing either mouse mammary carcinoma cells (4T1) or chinese hamster ovary cells (CHO) as scatterers. All scatterers were uniformly distributed spatially at random throughout the phantoms. Sound speed and attenuation were estimated in the phantoms versus temperature using insertion loss methods. Two parameters were estimated from the backscatter coefficient (effective scatterer diameter (ESD) and effective acoustic concentration (EAC)) and two parameters were estimated from the envelope statistics (k parameter and μ parameter) of the backscattered echoes versus temperature. The results of this study suggest that QUS has the potential to be used for noninvasive monitoring of temperature changes in tissues.**

I. Introduction

High intensity focused ultrasound has been suggested as a possible technique for clinical therapies involving noninvasive thermal ablation or hyperthermia. HIFU allows the targeting of small regions in thermal ablation or hyperthermia treatment and has been successfully demonstrated in animal models of cancer and in limited clinical studies and treatments. For successful HIFU treatments, a robust imaging and monitoring system is essential. In terms of monitoring the temperature rise in tissue treated with HIFU and guiding exposures, ultrasound, CT, and MRI have been examined [1]. However, currently only MRI has been found to accurately monitor and quantify the temperature rises in tissues treated with HIFU in vivo noninvasively and in the presence of tissue motion.

Ultrasound is an attractive imaging modality to guide and monitor HIFU treatment because it is non-ionizing, inexpensive, portable, real time, and convenient. Because of its attractiveness, several ultrasonic techniques have been investigated for monitoring, quantifying, and mapping the temperature rise induced in tissues by HIFU treatment. These techniques include quantifying changes in speed of sound and attenuation. As temperature increases in most tissues, the speed of sound also increases, which causes a slight time shift in backscattered echoes [2]. Quantitative ultrasonic techniques have been successfully used to characterize tissue microstructure [3]. Because the tissue microstructure changes during heating, ultrasonic backscattered energy, which is a function of tissue microstructure, may be used to stage, monitor and assess HIFU treatment.

The use of biophantoms to help develop QUS techniques for monitoring and assessment of HIFU therapy, to test new techniques, to assess performance of algorithms and measurement techniques, and identify mechanisms behind observations is essential. The use of biophantoms allows repeatable and controlled experiments to be conducted on materials that mimic living tissue. Work has been conducted to create biophantoms that will be good models for predicting in vivo behaviors. In the next sections experimental method and results are discussed in detail.

II. Experimental Methods

A. Biophantom Construction

Biophantoms were created using a 2% agar base doped with cells. Cells were used in the biophantoms because previous QUS studies have suggested that cells are an important feature giving rise to ultrasonic backscattered signals [3]. Several trial "recipe" formulations were attempted using cells in agar blocks to create useful biophantoms. In the first set of trials, cells were harvested from cell culture plates, spun in centrifuge tubes to separate the cells from the culture fluid, cells were extracted from the tubes, mixed and stirred gently into unsolidified agar at $45^{\circ}\mathrm{C}$, and then the agar was allowed to solidify (between $42^{\circ}\mathrm{C}$ and $43^{\circ}\mathrm{C}$) in cylindrical well plates. The concentration of cells in the biophantoms were between 4×10^6 to 5×10^6 per mL. Slices of the biophantoms were then examined under light microscope at various times after biophantom construction and the percentage of viable cells were estimated. In the initial trials, cell viability was less than 90% within twenty four hours of construction. Many of the cells were destroyed during the mixing process in the agar. A significant change in the recipe was to mix the cells in the agar solution with cell culture fluid. This change allowed cells to retain almost 50% viability within three hours of

biophantom construction. Therefore, all scans of biophantoms were conducted within three hours of construction.

B. Ultrasonic methods

The schematic of the experimental setup for assessing changes in biophantom scatterer properties versus temperature is shown in Fig. 1. A needle thermocouple was used to monitor the temperature with an accuracy of $1°\mathrm{C}$. The biophantom was completely submerged in a degassed water bath and a $20-\mathrm{MHz}$ single-element $f/3$ transducer was used for scanning. The transducer had a bandwidth of 10 to 28 MHz at -10 dB. A mechanical coil heater was used to heat the water, which also heated the phantom uniformly. The mechanical coil heater was controlled using a water bath temperature controller. Two types of phantoms were constructed and examined using ultrasound versus increases in temperature from 36 to $50°\mathrm{C}$ in $1°\mathrm{C}$ increments. The phantoms were biological phantoms made of agar and containing either 4T1 mouse carcinoma cells or CHO cells as scatterers. All scatterers were uniformly distributed spatially at random throughout the phantoms. A step size of 200 μm was used between consecutive scan lines. At each temperature value, 30 scan lines were acquired from different locations. Signals were recorded at every $1°\mathrm{C}$ increase in temperature in the phantoms.

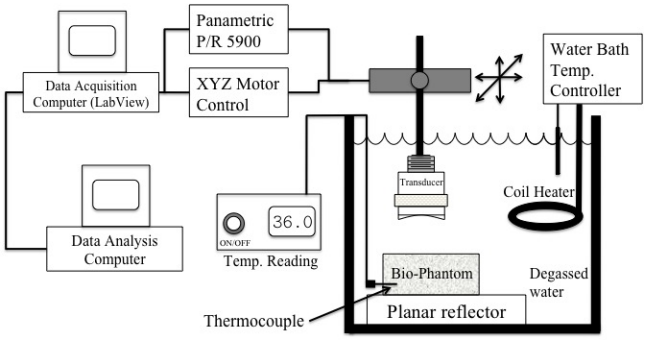

Fig. 1. Experimental setup.

Sound speed and attenuation were estimated in the phantoms versus temperature using insertion loss methods. The results are shown in Fig. 2. The estimates of sound speed increased monotonically in both phantoms from 1550 to 1580 m/s with increases in temperature. With increases in temperature the attenuation coefficients were observed to decrease by 0.05 dB/cm/MHz and 0.03 dB/cm/MHz in phantoms containing CHO and 4T1 cells, respectively. For speed of sound and attenuation calculations it was assumed that there were no significance increases/decreases in the material thicknesses which was also verified experimentally. The results also suggest that the attenuation was more sensitive to temperature variations than speed of sound.

Four cylindrical shaped bio-phantom containing CHO cells and four containing 4T1 cells were used for the QUS estimation experiments. B-mode images of the scanned areas were constructed. Regions of interest (ROIs) in the B-mode images

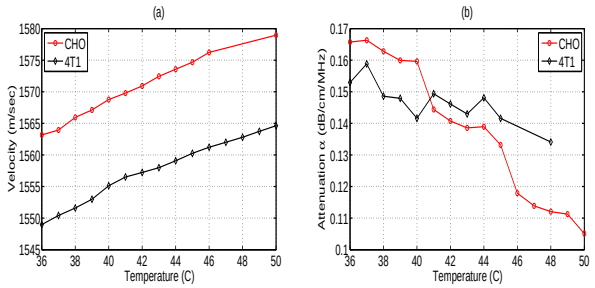

Fig. 2. Estimated (a) velocity and (b) attenuation.

were examined for the spectral content of the backscattered RF echoes. Square shaped ROIs of size 30λ by 30λ, (λ is the wavelength) were constructed. The backscatter coefficient (BSC) was estimated from the backscattered RF signals and a reference scan. The reference scan was obtained from a plexiglas planar reflector. Examples of the average BSC from all the ROIs versus temperature for the CHO and 4T1 biophantoms are shown in Fig. 3(a) and (b) respectively. The slope of the BSC curves changed with increases in temperature for both the phantoms.

The theoretical power spectrum is usually modeled according to the shape and distribution of scatterers postulated for the tissue. In soft tissue scattering, the spatial distribution of scatterers is assumed to be statistically stationary so that the distribution can be described in terms of a stochastic function, the spatial autocorrelation. In most cases of soft-tissue scattering, the Gaussian correlation function and associated form factor have been shown to describe tissue structures well. In the frequency domain using a Gaussian model the normalized, theoretical power spectrum is given by [4], [5]

$$W(f) = \frac{185 L q^2 a_{\mathrm{eff}}^6 \rho z_{\mathrm{var}}^2 f^4}{[1 + 2.66\,(f q a_{\mathrm{eff}})]} \exp\left[-12.159 f^2 a_{\mathrm{eff}}^2\right], \qquad (1)$$

where L is the gate length (mm), q is the ratio of aperture radius to distance from the region of interest, f is the frequency (MHz) and a_{eff} is the effective scatterer radius. The quantity, ρz_{var}^2 is termed the effective acoustic concentration (EAC) and is the product of the number of scattering particles per unit volume $\left(\mathrm{mm}^3\right)$, ρ, and the fractional change in the impedence between the scattering particles and the surrounding medium, $z_{var} = (Z - Z_0)/Z_0$, where Z and Z_0 are the acoustic impedance of the scatterers and the surrounding medium respectively. The effective scatterer diameter (ESD) and EAC are determined by comparing the measured normalized power spectrum from each ROI to a theoretical power spectrum shown in Eq. (1).

III. Results

Figures 4(a) and (c) show an enhanced B-mode images with superimposed pixels related to the ESD for CHO and 4T1 bio-phantoms, respectively at $36°\mathrm{C}$. The average ESD estimated for the CHO and 4T1 bio-phantoms were 18.7 μm and 35.5 μm, respectively. Similarly, Figs. 4(b) and (d)

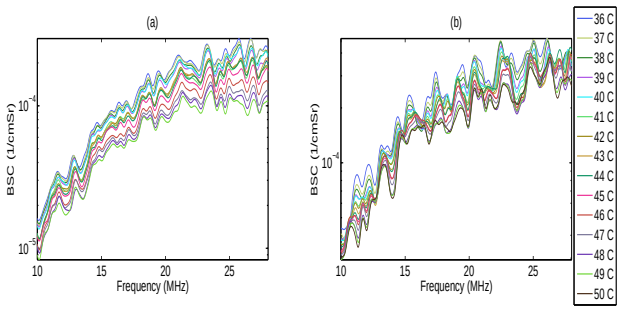

Fig. 3. Backscatter coefficient for bio-phantoms containing (a) CHO and (b) 4T1 cells.

represent enhanced B-mode images with superimposed pixels corresponding to the EAC for the CHO and 4T1 bio-phantoms, respectively. The average EAC estimated for the CHO and 4T1 bio-phantoms were 20.6 $\mathrm{dB/mm^3}$ and 12.8 $\mathrm{dB/mm^3}$, respectively. The enhanced B-mode images were constructed by using the attenuation values estimated at each particular temperature from the results shown in Fig. 2(b). The enhanced B-mode images reveal structures not observed in the ordinary B-mode images and could lead to improved detection and classification of diseased tissues. The uniformity of the colormap on the parametric images corresponds to the uniform distribution of cells in the bio-phantoms.

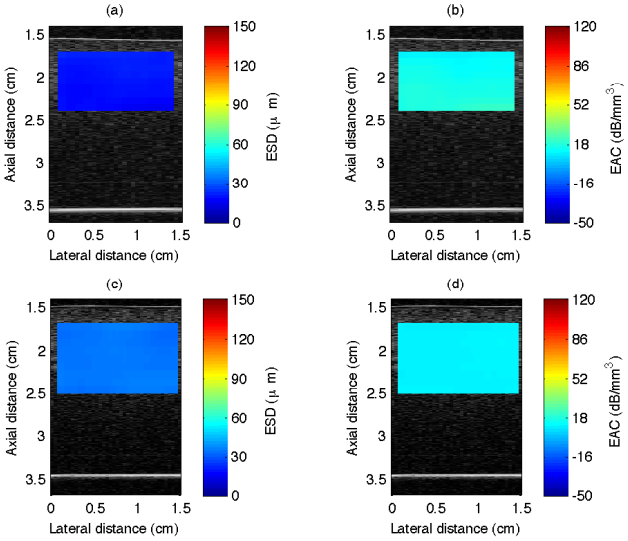

Fig. 4. Parametric images at 36°C with (a) ESD for CHO, (b) EAC for CHO, (c) ESD for 4T1, (d) EAC for 4T1.

Average estimates of ESD and EAC were calculated from four bio-phantoms containing each cell type. The estimated ESD ranged from 21 to 29 μm for CHO and 29 to 36 μm for the 4T1 phantoms at 36°C. The changes in ESD and EAC versus temperature with respect to the corresponding quantity at 36°C (i.e. $\Delta ESD(40°) = ESD(40°) - ESD(36°)$) are shown in Figs. 5 (a)-(d). A change of $5-10\%$ in the ESD for both the biophantoms over the temperature range was observed. The EAC was observed to change most dramatically of $20-40\%$ over the temperature ranges with a monotonically decreasing trend versus increasing temperature.

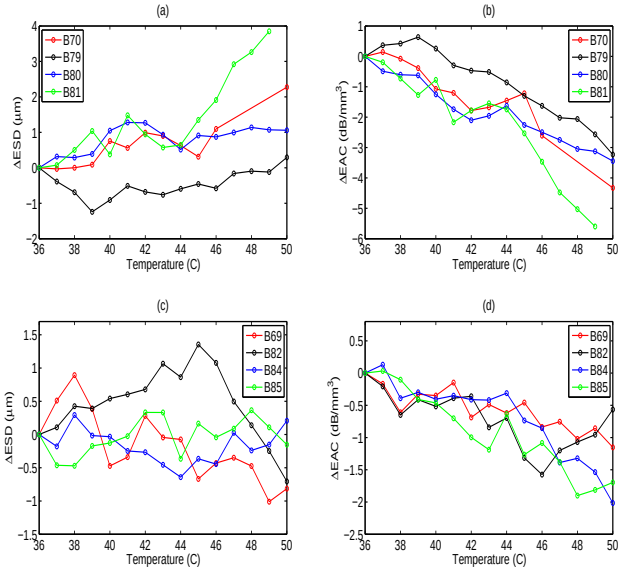

Fig. 5. Change in ESD and EAC with increase in temperature (a) ΔESD for CHO, (b) ΔEAC for CHO, (c) ΔESD for 4T1, (d) ΔEAC for 4T1.

Backscattered energy is proportional to the microstructure of the scattering media. Previous research has indicated that the backscattered energy depends on the organization of the cells in the tumor [6], [7]. Under a microscope it has been observed that 4T1 cells form clusters whereas the CHO cells do not. Organizational differences in cells were characterized using envelope statistics. The homodyned K distribution was used to model the amplitude of the envelope from ROIs in the bio-phantoms [8], [9]. The homodyned K distribution yields two parameters: the k parameter quantifies the randomness of the scatterer spacings and the μ parameter quantifies the number of scatterers per resolution cell. When the k parameter is zero, the scattering medium is considered to be truly random (Rayleigh distribution).

Estimates of the k parameter and the μ parameter were obtained from backscattered envelope signals corresponding to ROIs in the bio-phantom. Because the parameters corresponded to the same ROIs used to estimate the ESD and EAC, parametric images could be formed using the k and μ parameters shown in Fig. 6. From the parametric images the 4T1 cells were observed to have a higher number of scatterers per resolution cell than the CHO cells, which has also been observed in microscopic examination of these cell types.

The results from all the bio-phantoms at different temperatures are shown in Fig. 7. The results at any particular temperature represent the average quantity from all the ROIs from the particular bio-phantoms. The ROIs used for the envelop statistics analysis are exactly the same ROIs used to

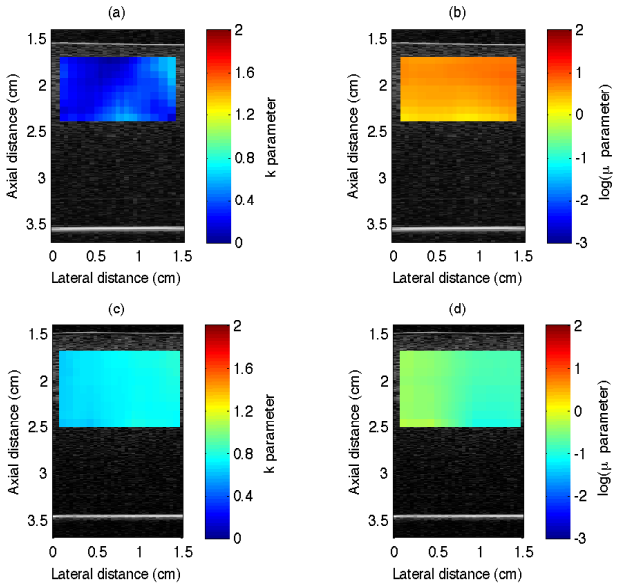

Fig. 6. Parametric images at 36°C with (a) k parameter for CHO, (b) μ parameter for CHO, (c) k parameter for 4T1, (d) μ parameter for 4T1.

estimate ESD and EAC previously. The results in terms of Δk and $\Delta\mu$ are the difference at a particular temperature with respect to the quantity at 36°C. Considering any particular bio-phantom the k and the μ parameters varied with increased heat, however, no specific trends were observed versus temperature.

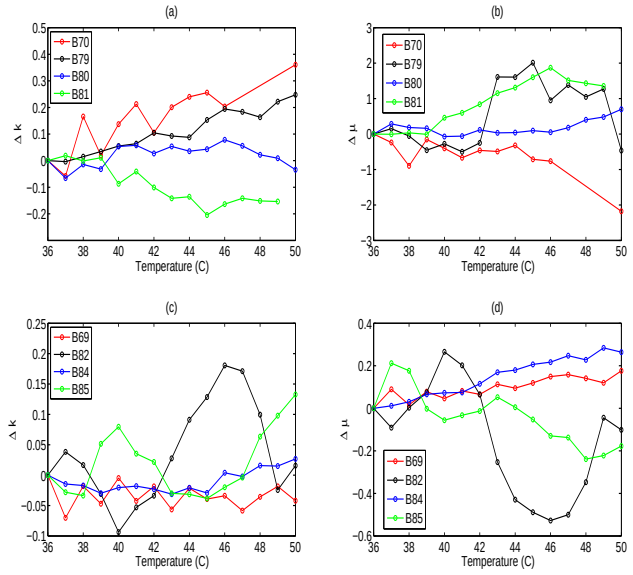

Fig. 7. Change in k and μ with increase in temperature (a) Δk for CHO, (b) $\Delta\mu$ for CHO, (c) Δk for 4T1, (d) $\Delta\mu$ for 4T1.

IV. Conclusion

Ultrasonic backscatter experiments were performed on two types of biological phantoms made of agar containing either 4T1 and CHO cancer cells, to understand the variations in QUS parameters with increases in temperature. A novel technique was developed to construct bio-phantoms such that the cells which represent scatterers had uniform distribution and random spatial locations throughout the phantom. These bio-phantoms were useful for performing controlled experiments with living cells. Each experiment lasted for 1.5-2 hours. It has been experimentally verified that the cells does not show any variations in the microstructure for 3 hours from the time of phantom construction. Therefore, all the variations in the QUS parameters are due to application of heat.

From the results it was observed that some QUS parameters were more sensitive to temperature changes than the others for a particular type of sample. The results suggest that the attenuation coefficient and EAC may be important quantities to monitor temperature variations. The similar characteristics of the ESD and EAC curves from four different phantoms for a particular cell type demonstrated the repeatability of this technique. Estimates of the k and μ parameters were obtained with increased temperature, which also exhibited variations with application of heat. The results of this preliminary study suggest that QUS has the potential to be used for noninvasive monitoring of temperature changes in soft tissues.

Acknowledgment

The authors would like to acknowledge the technical contributions of James P. Blue. The work was supported by NIH Grant R01-EB008992.

References

[1] G. T. Clement, "Perspectives in clinical uses of high-intensity focused ultrasound," *Ultrasonics*, vol. 42, pp. 1087–1093, 2004.

[2] J. C. Bamber and C. R. Hill, "Ultrasonic attenuation and propagation speed in mammalian tissue as a function of temperature," *Ultrasound Med. Biol.*, vol. 5, pp. 149–157, 1979.

[3] M. L. Oelze, J. F. Zachary, and W. D. O'Brien, Jr., "Parametric imaging of rat mammary tumors in vivo for the purposes of tissue characterization," *Journal of Ultrasound in Medicine*, vol. 21, pp. 1201–1210, 2002.

[4] M. F. Insana and T. J. Hall, "Describing small-scale structure in random media using pulse-echo ultrasound," *J. Acoust. Soc. Am.*, vol. 87, pp. 179–192, 1990.

[5] M. L. Oelze, J. F. Zachary, and W. D. O'Brien, Jr., "Characterization of tissue microstructure using ultrasonic backscatter: Theory and technique for optimization using a gaussian form factor," *J. Acoust. Soc. Am.*, vol. 112, pp. 1202–1211, 2002.

[6] Y. Saijo, M. Tanaka, H. Okawai, and F. Dunn, "The ultrasonic properties of gastric cancer tissues obtained with a scanning acoustic microscope system," *Ultrason. Med. Biol.*, vol. 17, pp. 709–714, 1991.

[7] A. S. Tunis, G. J. Czarnota, A. Giles, M. D. Sherar, J. W. Hunt, and M. C. Kolios, "Monitoring structural changes with a scanning acoustic microscope system," *Ultrason. Med. Biol.*, vol. 31, pp. 1041–1049, 2005.

[8] V. Dutt and G. F. Greenleaf, "Ultrasound echo envelope analysis using a homodyned k distribution signal model," *Ultrasonic Imag.*, vol. 16, pp. 265–287, 1994.

[9] M. L. Oelze, W. D. O'Brien, Jr., and J. F. Zachary, "Quantitative ultrasound assessment of breast cancer using a multiparameter approach," in *Proc. of the 2007 IEEE Ultrasonics Symposium*, 2007, pp. 981–984.